A COMPARATIVE STUDY OF MINERALOGICAL TRANSFORMATIONS IN FIRED CLAYS FROM THE LABOYOS VALLEY, UPPER MAGDALENA BASIN (COLOMBIA)

Oscar Mauricio Castellanos A.[1]; Carlos Alberto Ríos R.[2]; Miguel Angel Ramos G.[3]; Eric Vinicio Plaza P.[3]

ABSTRACT

Mineralogical transformations during firing of clays from the Laboyos Valley at the Upper Magdalena Basin (Colombia) were studied. Firing of clays was carried out in the temperature range 800–1200 °C under oxidizing conditions. The mineralogical transformations were investigated by X-ray diffraction (XRD) and scanning electron microscopy (SEM). Important compositional differences in the neoformed phases were observed in the clays. Typical assemblages with quartz, illite, kaolinite, mica, halloysite, potassium feldspar and plagioclase were observed. Several mineral phases were identified in the fired clays, with the reaction products including mullite, residual quartz, hematite, amorphous phase (glass generated by melting of feldspars and clays) in the fired clays.

Keywords: Mineralogical transformations, Clays, Laboyos Valley, Neoformed phases, Assemblages.

ESTUDIO COMPARATIVO DE LA TRANSFORMACIÓN MINERALÓGICA DE ARCILLAS COCIDAS DEL VALLE DE LABOYOS, CUENCA ALTA DEL MAGDALENA (COLOMBIA)

RESUMEN

Las transformaciones mineralógicas durante el quemado de las arcillas del Valle de Laboyos en la Cuenca del Alto Magdalena (Colombia) fueron estudiadas. La cocción de las arcillas se llevó a cabo en el rango de temperatura 800-1200 ºC bajo condiciones oxidantes. Las transformaciones mineralógicas fueron investigadas por difracción de rayos X (DRX) y microscopía electrónica de barrido (MEB). Importantes diferencias composicionales en las fases neoformadas se observaron en las arcillas. Paragénesis típicas con cuarzo, illita, caolinita, mica, feldespato potásico halloysita y plagioclasa fueron observadas. Varias fases minerales fueron identificadas en las arcillas quemadas, con productos de reacción incluyendo mullita, cuarzo residual, hematita, fase amorfa (vidrio generado por la fusion de feldespatos y arcillas) en las arcillas cocidas.

Palabras clave: Transformaciones mineralógicas, Arcillas, Valle de Laboyos, Fases neoformadas, Paragénesis.

[1] Programa de Geología, Universidad de Pamplona, Colombia, e-mail: **oscarmca@yahoo.es**
[2] Escuela de Geología, Universidad Industrial de Santander, A.A 678, Bucaramanga, Colombia
[3] Instituto Zuliano de Investigaciones Tecnológicas, Venezuela

INTRODUCTION

Clays are used as raw materials in many industrial fields, such as ceramics, paper, paint, petroleum industry, clarification of various effluents, catalysis (Chang, 2002). Their applications are tightly dependent upon their structure, composition, and physical attributes (Grim, 1960). The knowledge of these characteristics can help for best exploitation and eventually may open up new areas of application (Baccour *et al*., 2008). A wide range of clays have been used in the past in the manufacture of structural clay products (British Geological Survey, 2007). Clays are relatively common in many parts of the word and resources are, therefore, potentially very large. However, many types of clay are unsuitable for brick making. Clay is one of the most abundant natural mineral materials on earth. For brick manufacturing, clay must possess some specific properties and characteristics. A more complete knowledge of raw materials and their properties, better control of firing, improved kiln designs and more advanced mechanization have all contributed to advancing the brick industry.

Researchers are in a constant search to look for compositions, processing and microstructure property relationship for materials, by employing modern techniques such as X-ray diffraction and scanning electron microscopy. The brick vary in colour, compressive strength and water absorption. These are the characteristics which determine the durability of a brick and are related to its microstructure and mineralogy (Livingston *et al*., 1998). The durability of brick can vary significantly, depending both on the raw material itself and on the local environment (Bortz *et al*., 1990). According to Brindley and Maroney (1960), the durability of the brick, based on a visual assessment of distress, seemed related to the amount of cristobalite present (where cristobalite is a high temperature polymorph of quartz). As a general rule, bricks fired to high temperature (~1000°C), are more durable than those fired at low temperatures (Brindley and Maroney, 1960), which shows temperature dependence of brick's strength. The brick industry uses a great variety of clays, laid down at different geological periods. This geological diversity reflects itself in the varied composition and mineralogy of brick making clays (Jackson and Ravindra, 2000). The presence or absence of carbonates strongly influences the porosity development and therefore, the brick texture and physicalmechanical properties. The carbonates in the raw clay promote the formation of fissures and of pores under 1 μm in size when the bricks are fired between 800 and 1000°C (Robinson, 1982). The phosphate-bonded products are also of low porosity and improved dimensional stability. The properties of the phosphate-bonded clay bodies are critically affected by new mineral phases resulting from the reactions of phosphates with clay, which subsequently undergo physicochemical changes above 550°C (Cultrone *et al*., 1998). The important qualities of standard bricks are; adequate mechanical strength, well sintered with uniform colour, even surfaces and free of flaws or cracks with sharp and well defined edges, giving clear ringing sound when struck against each other, so hard that no impression is left when scratched with finger nails. In addition, they should absorb no more than 15% of its weight of water when kept immersed in it for 24 hours and should have a crushing strength more than 55kg/cm. Upon breaking, the surface should show a bright homogenous and compact surface free from voids or grit. A brick soaked in water for 24 hours should not show deposits of white salt on drying in shade (Bogahawatta and Poole, 1996).

The study of the temperature regime along the kiln indicates that the temperature in the preheating zone is below the prescribed value and in front of the firing zone it sharply increases, i.e., the rate of the temperature rise on this particular site exceeds the theoretical rate and the brick is subjected to an abrupt thermal shock, which impairs the quality of firing and increases the quantity of defects (Karim, 1998). Such defects include; bulges, non-uniform surface tint, metallic tarnish on bricks walls, cracks, decomposed brick or black core. The firing cycle begins with the drying to drive off the absorbed water (Dunham, 1992). The total time within the kiln varies between 24 to 48 hours during which the temperature gradually reaches typically to less than 1100ºC. Transformation of clay into brick can be divided into six stages (Dunham, 1992) including; dehydration of clay minerals, gypsum and iron oxide, loss of CO_2, sulphur and hydrocarbons, the alpha to beta quartz transformation, the solid-state mineral reactions, melt production and reactions upon cooling. The clay minerals illite, montmorillonite and halloysite also contain weakly bound water within their lattice structure, which is readily lost at 150 to 200ºC. The chemically bound water is evolved as the clay minerals themselves decompose between about 400ºC and 700ºC, leaving a residue of preponderantly noncrystalline material. Pyrite loses sulphur on heating by oxidation at around 400-450ºC (Brownell, 1976). Kaolinite is stable below 400ºC, however, above 400°C, the de-hydroxylation of kaolinite begins (Ghose, 2002).

Understanding of the brick microstructure as influenced by the range of temperature during firing cycle has been enhanced by the experimental on the

mineralogical transformations in fired clays (Ahmad *et al*., 2008), which are revealed by a series of evidences summarized below. A change in morphology from hexagonal platelets in kaolinite to pseudo-hexagonal flakes in metakaolinite occurs at approximately 550°C. Metakaolinite broken down at temperatures >900°C to γ-alumina-type spinel and a silica-rich phase. The spinel type phase started to transform into mullite at >1000°C. At 1300°C, mullite increased in size to ~1μm and in some regions, cristobalite formed from the silica-rich matrix (Lee *et al*., 1999; McConville and Lee, 2005). A number of phases are usually present in fired bricks. Quartz is observed in all samples, usually less abundant in the brick than in the raw material. Hematite is also present in all samples which impart the red colour to bricks. Even in yellow bricks, the presence of hematite is observed though in smaller amounts (Amjad, 2000). In addition to quartz, a number of other alkali silicate phases survive the firing cycle. In underfired bricks, illite is the most persistent of the clay minerals (Onike, 1985). Cristobalite has been noted as the most commonly occurring high temperature silica phase by some studies (Tuttle and Bown, 1958). The present study investigates the mineralogical transformation of clays from the Pitalito Basin, Huila (Colombia), which is very important to understand the technological properties of clay refractory products.

GEOLOGICAL SETTING

The Pitalito Basin is an intramontane basin situated at the junction of the Central and Eastern Cordilleras in the southern part of the Colombian Andes (FIGURE 1). Tectonic structures, evolution of the basin and distribution of the sediments suggest that the basin developed as a result of extension along a fault wedge which forms part of the Garzón-Suaza fault (Bakker *et al*., 1989). The basin can be divided into a relatively shallow western part (c. 300 m deep) and a deep eastern part (c. 1.200 m deep). The transition between both areas is sharp and is delineated by a NW/SE oriented fault. The position of this fault is reflected by the areal distribution of the deep non-exposed sediments as well as sediments at the surface: west of this fault the basin infill consists of coarse to medium elastics (conglomerates and sand) whereas in the eastern part fine elastics (clay and peat) are present. Sedimentologically, to the west there is an alternation of coarse material (gravel and sand) channel facies with fine material (clay and silt) facies overflow. To the east, numerous ridges or dikes shown high connection and many end in poorly drained areas. The dikes are composed of medium and coarse sand depressions deposits containing relatively thick peat and clay with thin interbedded sand. All these materials are known as Pitalito Fluvio-lacustrine Deposit (Cárdenas *et al*., 2003). The lateral transition between both types of sediment is abrupt and its position is stable in time. The surface and near surface sediments in the Pitalito Basin reflect the last stage of sedimentary infill which came to a halt between 17.000 and 7.500 years bp. These sediments were deposited by an eastward prograding fluvial system. The western upstream part of this system differs significantly from that of the eastern part which forms the downstream continuation. The western part exhibits unstable, shallow fluvial channels that wandered freely over the surface which predominantly consists of clayey overbank sediments. The alluvial architecture in the eastern half is characterized by stable channels and thick accumulations of organic-rich flood basin sediments and resembles an anastomosing river. The transition between both alluvial systems also coincides with the N/S oriented normal fault. Palaeoclimatic conditions over the last c. 61.500 years were determined by means of a pollen record.

According to Velandia *et al*. (2005), Pitalito Basin is structurally controlled by one of the six sectors of the Algeciras Fault System known as Altamira-Pitalito sector; the Pitalito pull-apart is a rhomboidal shape basin with a length of approximately 19 km; the flanks of this depression are marked by a fault arrangement that suggests an origin by the release produced by overstepping of right lateral faults; the Granadillo Fault bounds the Pitalito basin to the north and is interpreted as a synthetic structure of the main fault system; a small lazy-S shaped basin is located to the SW vertex of the Pitalito pull-apart; this lazy-S basin is interpreted as having been fashioned by a releasing bend of the westernmost fault of the system. Fluvial-lacustrine and alluvial deposits accumulated in this small basin indicate that the westernmost fault of the system was active before the easternmost fault. The straight line of the Pitalito Fault suggests a high-angle structure, although associated with satellite faults, which show lower angles forming wedges or lenses on either side of the main fault. In the southern part it constitues the contact between the Saldaña Formation and Sombrerillos Quartz-monzodiorite (Cárdenas *et al*., 2003).
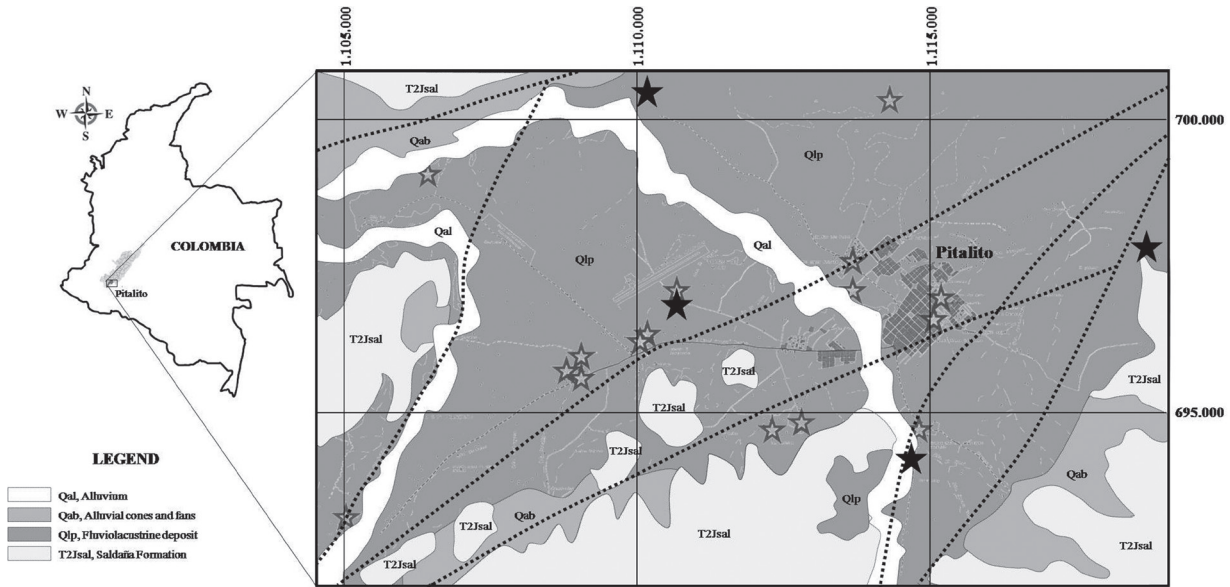
FIGURE 1. Localization of the studied area, the Pitalito basin (Colombia). Localization of sampling sites, showing the tested samples (black stars).

EXPERIMENTAL PROCEDURE

Materials

Clays are natural materials that cannot be considered pure minerals as they contain some impurities such as quartz, feldspars or other clay types in minor amounts. The raw clays used in this study were collected by Castellanos (2005) from the fluvio lacustrin deposit of Pitalito of Quaternary age of the Laboyos Valley at the Upper Magdalena Basin (Colombia) during a geological characterization of this clay deposit. A detailed geotechnical characterization of these clays according to the ASTM standards has been summarized by this author. Clays from this site, which are used in brick industry, were investigated in their natural state and after calcination at different temperatures.

Experimental procedure

A set of samples, including unfired and fired clays, was subjected to petrographic analysis (using a NIKON Eclipse 50i POL transmitted light microscope), in order to carried out mineralogical characterization. The samples were initially impregnated by immersion in a pot containing Epo-tek resin, mixed with blue dye powder. The addition of blue dye ensures that any fracturing or porosity inherent to the sample (as opposed to damage caused by slide preparation) is preserved on the thin section. As a result of this analysis, the percentages of silt-size inclusions plus the species, sizes, and percentages of mineral inclusions of sand size and larger were ascertained and used to characterize the physical composition of each thin section. During this stage, precautions were taken to ensure that each thin section was analyzed "blind." That is, all petrographic observations were made without knowledge of the ceramic type of any specimen.

Powder X-ray diffraction was carried out to determine the mineralogical composition of the samples, using a Philips PW1710 diffractometer operating in Bragg–Brentano geometry with Cu-Kα radiation (40 kV and 40 mA) and secondary monochromation. Data collection was carried out in the 2θ range 2–50°, with a step size of 0.02°. Phase identification was performed by searching the ICDD powder diffraction file database, with the help of JCPDS (Joint Committee on Powder Diffraction Standards) files for inorganic compounds.

The morphology of the raw materials and as-synthesized zeolites was examined by environmental scanning electron microscopy (FEI Quanta 200), under the following analytical conditions: magnification = 100-6000x, WD = 7.0 mm, HV = 8.4 kV, spot = 3.0, signal = SE, detector = LFD. Powder samples of the raw clays, obtained in an agata mortar, were used to produce miniature bricks or briquettes (prismatic samples of 8,2 cm × 4.1 cm × 1,8 cm), which were manufactured by hand moulding in the laboratory.

The small-scale bricks were considered as a first step to spot if the laboratory results would encourage shifting to an industrial scale. The scale effect would affect

mostly the strength of the bricks; that is why we should aim a higher compressive strength. The briquettes were dried at room temperarure and then thermally treated in a laboratory programmable furnace at different temperatures (800, 900, 1000, 1100 and 1200 °C), in an oxidizing atmosphere. Then they were quenched by air to ambient temperature. The dehydrated materials were subsequently subjected to chemical characterization. The treated small-scale bricks were used for testing.

RESULTS AND DISCUSSION

Effect of firing temperature

The effect of firing temperature on the colour and shrinkage of the clay are illustrated in FIGURE 2. As revealed by this figure, there are interesting changes in the appearance of tested briquettes, which are going to be discussed in detail as follows. First of all, a variation of the color tonality after firing is revealed, which is particularly associated to the chemical composition of the raw clays. Color gets darker for increasing temperature due to the high concentration of iron oxides content (Swapan *et al.*, 2005). Drastic changes occur between 1000 and 1200 °C, temperature range within all samples showed a transformation from a baked material to a vitrified material. The best results of firing clay between 800 and 1000 °C, although in some cases crude tones in fired clays were observed. The best results of vitrification occurred at 1100 °C.
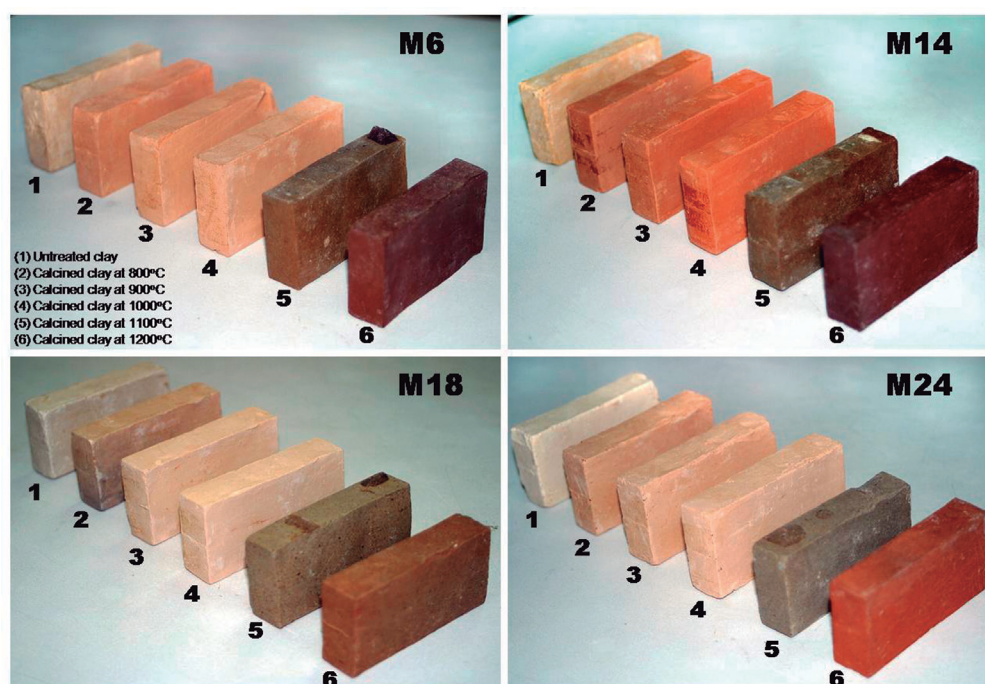
FIGURE 2. Effect of firing temperature on the colour and shrinkage of the clay.

Using a Munsell Color Chart, the briquettes were designated into categories according to color (TABLE 1). Raw clay-based briquettes display pink, pinkish white and grey colors. On the other hand, the fired briquettes show pink, light brown, dark brown, very dark brown, strong brown, brown, dark grey and very dusky red colors. Results reveal both the variability within a single firing and between firings. According to Stępkowska and Jefferis (1992), firing colour of clays seems to be influenced by clay microstructure. Non- or slightly expandable parallel arrangement and stiff particles, prevent Fe^{2+} oxidation and result in a yellow colour. In the presence of Na the clay matrix becomes dark coloured on firing whereas grains of parallel structure remain yellow. The raw materials can present different Fe content, which can also explain a variation of the tonality of the color after firing. Fe is generally present in clay minerals which later in firing are responsible for the formation of mullite. The color tends to be darker even if they contain a lower quantity of transition elements, which is due to the presence of goethite, which can be rapidly decomposed into hematite with temperature, and the low content of newly formed mullite, which could eventually host Fe in the structure (Ferrari and Gualtieri, 2006).

TABLE 1. Color categorization

Laboratory briquette	Munsell hue page	Munsell classification
M6	7.5P	8/4
M6-800	7.5LB	6/4
M6-900	7.5P	7/4
M6-1000	7.5P	7/4
M6-1100	7.5DB	3/2
M6-1200	7.5VDB	2.5/3
M14	7.5P	8/4
M14-800	7.5SB	5/8
M14-900	7.5SB	5/8
M14-1000	7.5SB	5/8
M14-1100	7.5DB	3/2
M14-1200	7.5VDB	2.5/3
M18	7.5G	6/1
M18-800	7.5B	5/3
M18-900	7.5P	8/4
M18-1000	7.5P	8/4
M18-1100	7.5B	4/2
M18-1200	10VDR	2.5/2
M24	7.5PW	8/2
M24-800	7.5LB	6/3
M24-900	7.5P	7/4
M24-1000	7.5P	7/4
M24-1100	7.5DG	4/1
M24-1200	10VDR	2.5/2

P, pink; LB, light brown; DB, dark brown; VDB, very dark brown; SB, strong brown; G, grey; B, brown; PW, pinkish white; DG, dark grey; VDR, very dusky red.

Mineralogical composition

Petrographic findings. For the refractory bricks differentiation, surface texture and intensity (FIGURE 3) have been found as immediately obvious distinctive features between these materials. We attempted to identify and differentiate bricks varieties solely by analysis of surface texture, which however was not an effective alternative.

The petrography of the unfired and fired clays shows them to be variable (FIGURE 4). Raw clays (FIGURE 4a) show few clasts up to coarse silt in size or significant amounts of coarse sand size clasts. They typical show a red clay matrix, with rounded inclusions of black silty clay and black non-silty iron oxide rich material. All of the fired test-pieces contain areas with a different firing colour from that of the main clay. They contain rounded,

petrographically opaque aggregates of black silty clay or black, non-silty material. In these aggregates silty, silicate inclusions are mainly arranged at random, but there are some examples showing a concentric arrangement; the opaque aggregates (and probably also the black layering referred to above) might be iron oxide-rich, or they could represent incompletely burned-out organic material (Carney, 2010). The fired clays consist of various fragments embedded in a thermally transformed clayey matrix. The fragments within the matrix are regarded as non-plastic components, which occur in variable amounts and consist of clasts of different materials (FIGURES 4b-4f). The degree of vitrification increases gradually up to almost complete melting resulting in a glassy appearance. Among the crystalloclasts, quartz is predominant, followed by feldspar and hematite. Several studies reveal that quartz, plagioclase, K-feldspar, muscovite, rare biotite and occasionally minerals, such as amphibole, pyroxene, garnet, epidote-zoisite, titanite, zircon, rutile, ilmenite, apatite and tourmaline (e.g., Ghergari *et al.*, 2003; Horga, 2008). Quartz displays molten rims with some invasion of Fe-oxides. Further determination in terms of mineral composition is not possible. The feldspars are almost homogenous optically and show only cleavage and twinning as characteristic features. The matrix has different appearances due to the development of hematite where it can be recognized as few small crystals dispersed in a uniform red Fe-rich surface.

X-ray powder diffraction. FIGURE 5 illustrates the changes of the XRD diffractograms of clay samples from the Laboyos Valley with increasing temperature. The inter-planar spacing corresponding to XRD peaks observed for the starting clays matched as follows: FIGURE 5a shows the occurrence of quartz (PDF 33-1161), albite (PDF 89-6424), microcline (PDF 77-135), illite (PDF 26-911), halloysite (PDF 29-1489) and muscovite (PDF 1-1098) in clay M6. As shown in FIGURE 5b, the mineral phases detected in clay M14 were quartz (PDF 33-1161), albite (PDF 89-6424), microcline (PDF 77-135) and orthoclase (PDF 22-1212). In clay M18 (FIGURE 5c) were observed quartz (PDF 86-1630), albite (PDF 89-6424), microcline (PDF 19-932) and illite (PDF 26-911). The mineral phases detected in clay M24 were quartz (PDF 85-460), albite (PDF 89-6424), microcline (PDF 19-932), illite (PDF 26-911), halloysite (PDF 29-1489) and sodalite (PDF 85-2065) as indicated in FIGURE 5d. These results reveals that illite, halloysite and muscovite appear to be the primary clay minerals in the clay samples, and quartz as the major non-clay mineral (as revealed by the XRD peak intensity), with traces of different mineral phases like high, ordered and low albite, orthoclase and intermedie microcline (wide reflections with low intensity).
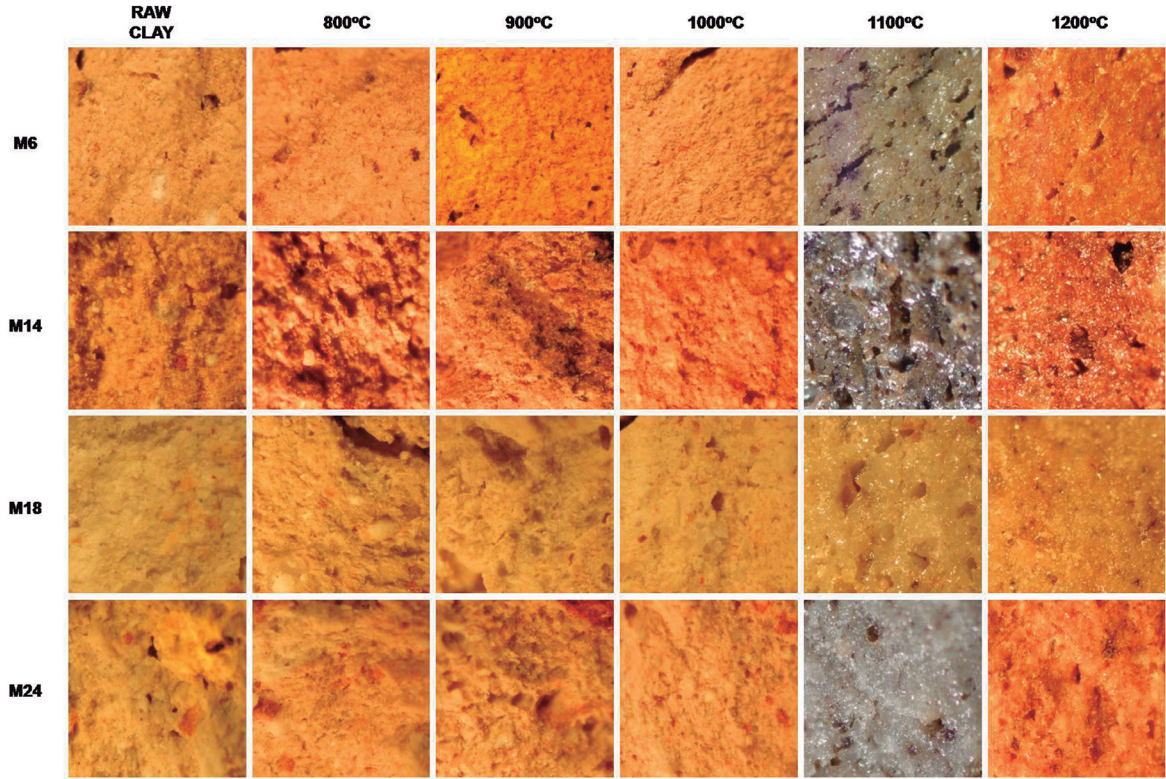
FIGURE 3. Photographs of the test briquettes under the binocular stereomicroscope.
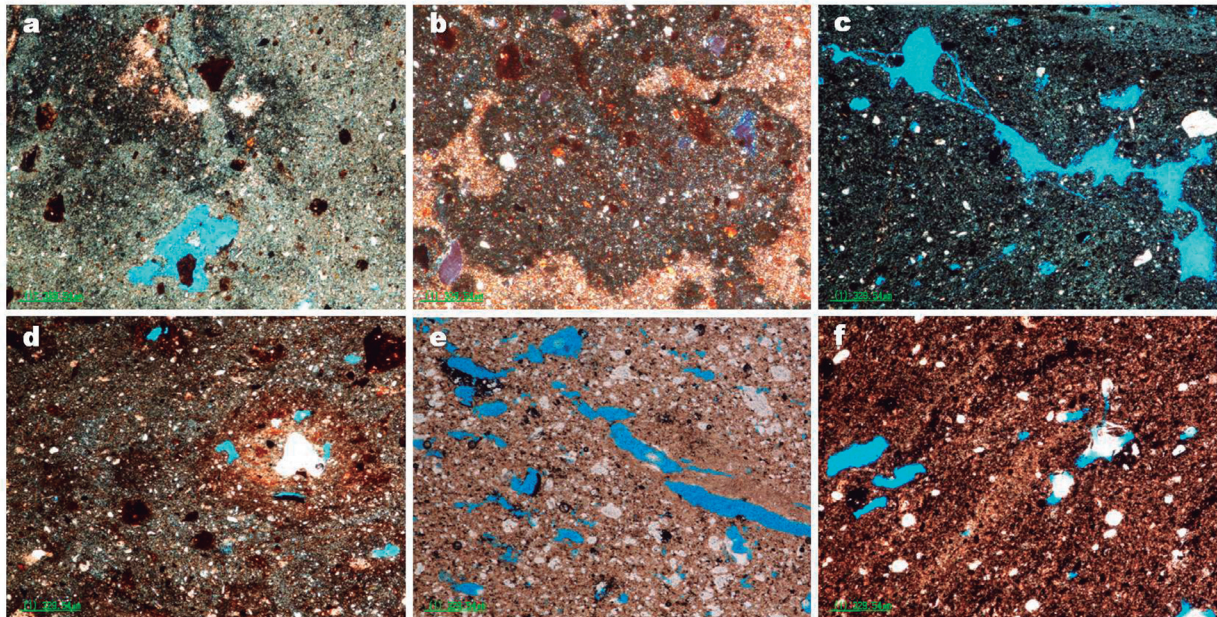
FIGURE 4. Petrographical features of unfired and fired clays.

On the other hand, in the fired clays (FIGURE 5) residual quartz, albite and microcline, along with mullite (PDF 89-2645) and hematite (PDF 33-664) were detected. The diffractograms remained relatively unchanged up to 900 or 1000 °C. High-intensity reflections attributed to quartz progressively decrease in intensity with heating temperature. The mineral clays, such as illite, become progressively less crystalline and the intensity of their

lines gradually decreases and disappears between 900 and 1000 °C. The XRD peaks of the residual clay phases remain with a similar intensity at this temperature range, whereas mullite XRD peaks begin to emerge between 1000 and 1100 °C from the background of the crystalline clay reflections. As the temperature reaches 1200 °C, the intensity of the mullite peaks obviously increases, with the appearance of hematite.

In general, a significant change was observed when clays were fired from 1000 to 1200 °C. Along with the disappearance of the lines of quartz and a decrease in the feldspar content is noted. According to Trindade *et al*. (2009), quartz decomposes gradually from 800 to 1100 °C, diminishing drastically at 1100 °C. Orthoclase peak was slowly diminishing when fired from 1000 to 1100 °C and completely disappeared at 1200 °C, which can be attributed to the formation of mullite (Johari *et al*., 2010) between the temperatures of 1000 to 1200 °C. The characteristic peaks also became sharp, showing a highly crystalline phase. Similar results have been reported in previous studies (Jordan et al., 2008; Chindraprasirt and Pimraksa, 2008; Trindade *et al*., 2009; Johari *et al*., 2010).
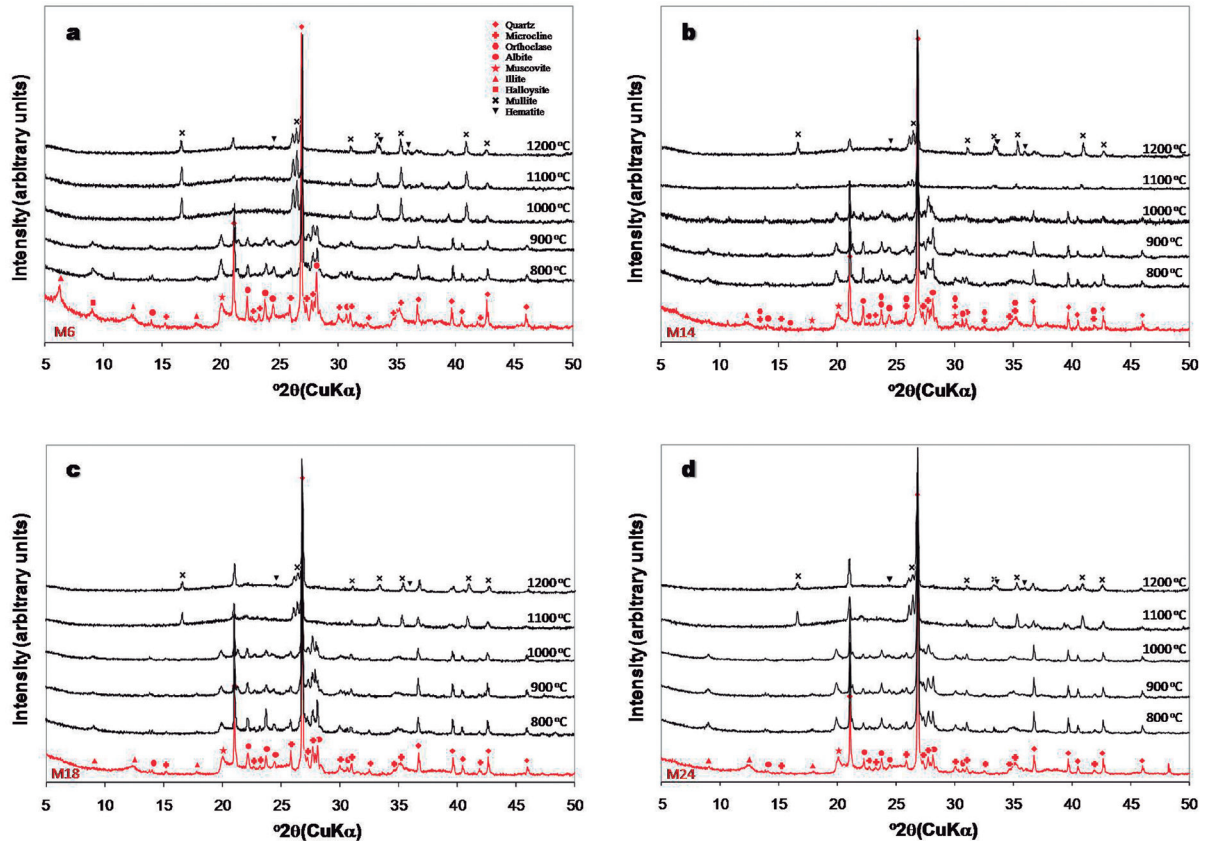
FIGURE 5. Representative X-ray powder diffraction patterns of the unfired (red color) and fired clay at different temperatures.

The formation of hematite at 1200 °C as a new mineral phase should be considered in future studies at higher temperature, taking into account that the XRD peaks of hematite become gradually more intense with increasing fire temperature as reported by Hua *et al*. (2004). However, results from Trindade *et al*. (2009) reveal that hematite can be identified at 500 °C, whereas well-crystallized hematite is a significant component only at a temperature of 900 °C. A very important fact that can be observed with increasing temperature is the complete disappearance of some mineral phases and the diminishing of the remaining, as suggested by the decrease in the intensity of the diffraction maximum or rising of the background noise, suggesting the presence of an amorphous phase similar to what is reported by Trindade *et al*. (2009). At this step the clay body would essentially be an amorphous material with some residual compounds, and neoformed mullite and hematite. XRD

data reveal that the decomposed and disappearing phases all contribute to the formation of an amorphous phase above 1000 °C, and besides mullite (at 1000 °C) and hematite (at 1200 °C) formation no new crystalline phases appeared.

Scanning electron microscopy. SEM photomicrographs exhibit the microstructure differences between unfired and fired at different temperatures clays (FIGURE 6). The microstructure changes with the sintering temperature. These differences result from transformations in the clay matrix, in mineral phases and at boundaries between clay matrix and mineral phases, as reported in other studies (e.g., Riccardi *et al.*, 1999). Crystalline phases are embedded in a vitreous phase. The nucleation mechanism of new phases involves the consumption of quartz and clay minerals. At 800 °C and 900 °C, the briquettes have not yet experienced full solid state sintering process since the individual clay particles are still existent, which is in agreement with that reported by Johari *et al.* (2010). Tite and Maniatis (1975) showed that the brick structure formed at lower temperatures (840-960 °C) remained essentially the same until temperaturas of over 1080 °C

are reached. The fracture surface looks rough and a bit dusty. According to Johari *et al.* (2010), bricks that were sintered until 1000 °C can be considered as having a porous structure. A secondary bubbles formation due to the extensive melting of clay particles in the matrix was observed. Pores are ellipsoid with smooth edges and coalesce resulting in the so-called cellular structure (Tite and Maniatis, 1975). Interconnectivity among particles is extensive. Between 1000 and 1100 °C, the solid state sintering should become very significant since raw clays had been fully sintered and very few pores can be seen in the microstructure.

The solid state sintering is a process that promotes atomic bonding between particles by a diffusion mechanism (Barsoum, 1997). This diffusion followed by grain growth will create a dense structure with significant shrinkage, causing the reduction in volume for brick sintered within this range of temperature (Johari *et al.*, 2010). The briquettes sintered between 1100 and 1200 °C have a glassy appearance and therefore vitrification can be clearly detected. The optimum temperature of the sintering process is reached at 1200 °C and whereby its microstructure contains minimum pores (Johari *et al.*, 2010).
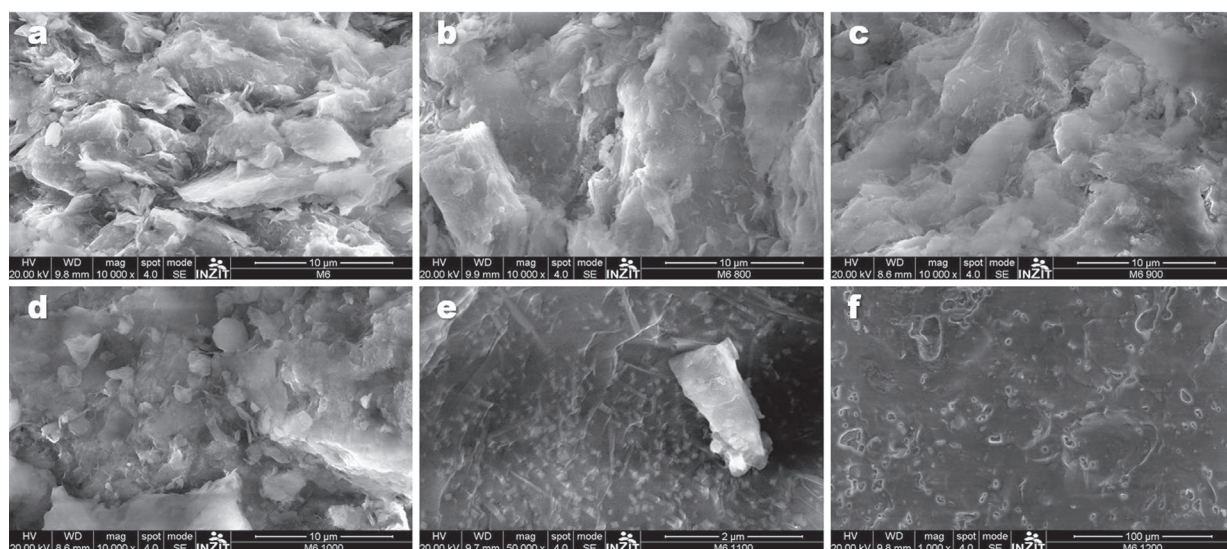
FIGURE 6. SEM images of representative (a) unfired and (b-f) fired clay brickettes.

Mineral transformations. In general, quartz is the most common mineral phase in the raw materials; the other components are phyllosilicates and feldspars. The < 2 mm fraction includes illite, smectite and low amounts of kaolinite. Firing causes significant changes in the phyllosilicates. By comparing the firing behaviour of the natural clays used in this study, it is clear that the thermal reaction paths are quite different, but similar phases are formed towards the stage of stable products.

During heating three kinds of processes take place: decomposition, phase transformation, and sintering with partial melting, with both decomposition and phase transformations affect development and extent of the subsequent sintering (Baccour *et al.*, 2008).

As demonstrated in previous studies (e.g., Cultrone *et al.*, 2001), firing up to 700 °C induce no significant mineralogical/textural transformations. Clay minerals

structure is reported to collapse due to dehydroxylation to an illite-like structure when a temperature between 450 and 550 °C is reached (Evans and White, 1958). A dehydroxylated phyllosilicate phase, structurally different to the hydrated one (Guggenheim *et al.*, 1987), is reported to exist up to 950 °C when complete breakdown of the dehydroxylated illite occurs (Peters and Iberg, 1978). According to Cultrone *et al.* (2001), the dehydroxylation process is not completed at T ~ 900 °C, which indicates that the kinetics of this process is slower than previously estimated by Evans and White (1958).

The phases present between 800 and 900 ºC were illite, muscovite, halloysite, quartz, potassic feldspar and plagioclase. At this temperature, the crystalline structures of chlorite and kaolinite were affected but not illite, which probably decomposed between 900 and 1000 ºC.

At 900 ºC illite, muscovite, halloysite, quartz, potassic feldspar and plagioclase were the major phases detected. The crystalline of kaolinite were affected but not illite. Nevertheless, at 1000 ºC, neomineralizations of mullite and hematite occurred which can be attributed to the mineral dynamics invoked by the thermal process.

At 1100 ºC, the most significant difference between the fired clays is the appearance of mullite between 1000 and 1100 ºC. Mullite may appear at different temperature, which could be related to the presence of enough content of illite/sericite. At this range of temperature, phyllosilicates have already disappeared in all samples, being transformed into mullite plus a melt (Cultrone *et al.*, 2001). We assume that mullite is formed in the temperature range of 1000-1100 ºC, increasing in concentration as the temperature rises. Other mineral phases also increase in concentration as the temperature rises, such as hematite, with iron being trapped in the network of the aluminosilicates and, therefore, the formation of hematite is inhibited (Maniatis *et al.*, 1981). There is not evidence that favours the presence of spinel phase rather direct mullite formation. The interpretation of mullitization proposed by Aras (2004) is that is the first spinel phase and the amorphous components formed and then reacted at 1100-1150 ºC to form mullite. Variables affecting the mullite formation include type of flux, level of alkalis, kaolinite content, possible occurrence of melted phases, and Fe impurities and atmosphere particularly in Fe-containing systems (Lee *et al.*, 2008; Pardo *et al.*, 2011). These variables influence mullite and other phase formation by affecting the composition and viscosity of the liquid in which it grows. According to Aras (2004), feldspar melting is strongly influenced by the original mineralogy of clays and more cristobalite formation is favoured in Ca-Na feldspar fired clays than in K feldspar fired clays. The percentage of newly formed mullite and residual quartz content are inversely correlated to the quantity of amorphous phase (glass generated by melting of feldspars and illite) in the fired bodies (Ferrari and Gualtieri, 2006). According to them, quartz is unstable in the alkaline melt and tends to decompose whereas mullite formation is inhibited, because of the depletion of Al and Si ingested in the alkaline glass.

The major phases between 1100 and 1200 ºC were mullite, hematite and residual quartz. Feldspars were only identified in the natural clay as residual compounds. Quartz decomposes gradually from 800 to 1100 °C, diminishing drastically at 1100 °C, and disappeared at 1200 ºC. The decomposed and disappearing phases all contribute to the formation of a vitreous phase up to 800 °C. At this step the clay would essentially be an amorphous material with some residual grains of quartz and neoformed mullite and hematite and other high temperature mineral phases such as microcline. Therefore, quartz was a residual phase, i.e. a component of the raw clay that did not suffer chemical transformations during the firing stage, except at 1200 ºC. On the contrary, mullite, hematite and other silicates were formed during firing. Clays showed phyllosilicate destruction at temperature ranging from 700 to 900 °C, followed by vitrification which is significant at temperature > 1000°C.

CONCLUSIONS

The major phases present in the raw clays are quartz, illite, kaolinite, mica, halloysite, potassium feldspar and plagioclase. Several mineral phases were identified in the fired clays, with the reaction products including mullite, residual quartz, hematite, amorphous phase (glass generated by melting of feldspars and clays) in the fired clays. A fluid texture analogous to that in porphyritic type rocks was observed in which quartz phenocrysts occur in the partially microcrystalline matrix. The color of the fired clays tends to be darker at higher temperature, which can be related to the presence of goethite, which can be rapidly decomposed into hematite with temperature, and the low content of newly formed mullite, which could eventually host Fe in the structure. Results reveal the persistence of illite up to at least 900ºC during firing. Increasing content of illite in the mixtures determines a decrease of mullite, cristobalite and quartz in the fired products. Free alumina and silica are depleted

for the formation of the alkaline glass and quartz is unstable in the alkaline melt. Knowledge of the mineralogical phase composition of the raw materials used for the preparation of bricks is very importance for understanding of the technological properties of clay refractory products.

ACKNOWLEDGMENTS

REFERENCES

Ahmad, S., Iqbal, Y., and Ghani, F. 2008. Phase and Microstructure of Brick-Clay Soil and Fired Clay-Bricks. From Some Areas in Peshawar Pakistan. Journal of The Pakistan Materials Society, 2(1): 33-39.

Amjad, J. 2000. Investigation of phases in soils used for brick-making. M.Phil. Thesis, University of Punjab, Lahore (Pakistan).

Aras, A. 2004. The change of phase composition in kaolinite- and illite-rich clay-based ceramic bodies. Applied Clay Science, 24(3-4): 257-269.

Baccour, H., Medhioub, M., Jamoussi, F., Mhiri, T., and Daoud, A. 2008. Mineralogical evaluation and industrial applications of the Triassic clay deposits, Southern Tunisia. Materials Characterization, 59(11): 1613-1622.

Bakker, J.G.M., Kleinendorst, T.W., and Geirnaert, W. 1989. Tectonic and sedimentary history of a late Cenozoic intramontane basin (The Pitalito Basin, Colombia). Basin Research, 2(3): 161-187.

Barsoum, M.W. 1997. Fundamental of Ceramics. McGraw-Hill, Singapore, 603p.

Bogahawatta, V.T.L., and Poole, A.B. 1996. The influence of phosphate on the properties of clay bricks. Applied Clay Science, 10(6): 461-475.

Bortz, S.A., Marusin, L.S., and Monk, C.B. Jr. 1990. A critical review of masonry durability standards. Proceedings of the 5th North American Masonry Conference, Illinous, USA, pp. 1523-1536.

Brindley, G.W., and Maroney, D.M. 1960. High–temperature reactions of clay mineral mixtures and their ceramic properties: II, Reactions of Kaolinite-Mica-Quartz Mixtures Compared With the $K_2O-Al_2O_3-SiO_2$ Equilibrium Diagram. Journal of the American Ceramic Society, 43(19): 511-516.

British Geological Survey 2007. Brick clay: Geology and mineral planning factsheets for Scotland. Consulted on March 21 2010. http://www.scotland.gov.uk/Publications/2007/06/04121200/1

Brownell, W.E. 1976. Structural clay products. Springer-Verlag, New York, 231p.

Cardenas, J.I., Núñez, A., and Fuquen, J.A. 2003. Geología de la Plancha 388 Pitalito – Memoria Explicativa. INGEOMINAS. Bogotá, Colombia, 128p.

Carney, J.N. 2010. Comparative petrography of pottery sherds and potential geological source materials in the East Midlands. Open Report of the British Geological Survey, OR/10/034.

Castellanos, O. (2005). Caracterización geológica de arcillas del Valle de Laboyos, Municipio de Pitalito, Huila. Bistua, 3(2): 43-53.

Chang, L.L.Y. 2002. Industrial mineralogy: Materials, processes, and uses. Prentice Hall, New Jersey, 472p.

Chindraprasirt, P., and Pimraksa, K. 2008. A study of fly ash-lime granule unfired brick. Powder Technology, 182(1): 33-41.

Cultrone, G., Sebastian, E., Cazalla, O., and de la Torre, M.J. 1998. Physical, mineralogical and textural features of ceramic clays from Granada Province (Spain). Proceedings of the 2nd Mediterranean Clay Meeting, Aveiro, Portugal, pp. 298-303.

Cultrone, G., Rodriguez-Navarro, C., Sebastian, E., Cazalla, O., and de la Torre, M.J. 2001. Carbonate and silicate phase reactions during ceramic firing. European Journal of Mineralogy, 13(3): 621-634.

Dunham, A.C. 1992. The mineralogy of brickmaking. Proceedings of the Yorkshire Geological Society, The Geological Society, London, United Kingdom, pp. 95-104.

Evans, J.L., and White, J. 1958. Further studies of the thermal decomposition of clays. Transactions of the British Ceramic Society, 57: 289-315.

Ferrari, S., and Gualtieri, A.F. 2006. The use of illitic clays in the production of stoneware tile ceramics. Applied Clay Science, 32(1-2): 73–81.

Ghergari, L., Ionescu, C., and Horga, M. 2003. Mineralogy of ceramic artefacts from Ilişua archaeological site (Bistriţa-Năsăud County, Romania. Studii şi Cercetări Geologie-Geografie, 8: 129-137.

Ghose, D.N. 2002. Materials of Construction, Tata McGraw Hill, New Delhi, India, 296p.

Grim, R. 1960. Some applications of clay mineralogy. American Mineralogist, 45(1-2): 259-269.

Guggenheim, S., Chang, Y., and van Groos, A.F.K. 1987. Muscovite dehydroxylation: high-temperature studies. American Mineralogist, 72: 537-550.

Horga, M. 2008. Geoarchaeological studies on ceramics and lithics from archaeological sites from Bistriţa-Năsăud County, Romania). Ph.D. Thesis, Babeş-Bolyai University of Cluj-Napoca.

Jackson, N., and Ravindra, K.D. 2000. Civil Engineering and Materials. Mac-Millan Education Press, London, United Kingdom, 534p.

Johari, I., Said, S., Hisham, B., Bakar, A., and Ahmad, Z.A. 2010. Effect of the Change of Firing Temperature on Microstructure and Physical Properties of Clay Bricks from Beruas (Malaysia). Science of Sintering, 42: 245-254.

Jordan, M.M., Montero, M.A., Meseguer, S., and Sanfeliu, T. 2008. Influence of firing temperature and mineralogical composition on bending strength and porosity of ceramic tile bodies. Applied Clay Science, 42(1-2): 266-271.

Hua, J., Wei, K., Zheng, Q., and Lin, X. 2004. Influence of calcination temperature on the structure and catalytic performance of Au/iron oxide catalysts for water–gas shift reaction. Applied Catalysis A: General, 259(1): 121-130.

Karim, F. 1998. Ceramics & Plastics: Testing of Engineering. Ferozsons, Lahore, Pakistan, 256p.

Lee, W.E., Souza, G.P., McConville, C.J., Tarvornpanich,

T., and Iqbal Y. 2008. Mullite formation in clays and clay-derived vitreous ceramics. Journal of the European Ceramic Society, 28(2): 465–471.

Lee, S., Kim, Y.J., and Moon, H.S. 1999. Phase transformation sequence from kaolinite to mullite investigated by an energy-filtering transmission electron microscope. Journal of the American Ceramic Society, 82(19): 2841-2848.

Livingston, R.A., Stutzman, P.E., and Schumann, I. 1998. Quantitative X-Ray Diffraction Analysis of Handmolded Brick. In: Foam Conservation of Historic Brick Structures - Chapter 11 (Eds. Shafesburg, U.K., Baer, N.S., Fritz, S., and Livingston, R.A.), Donhead Publishing Ltd., pp. 105-116.

Maniatis, Y., Simopoulos, A., and Kostikas, A. 1981. Moessbauer study of the effect of calcium content in iron oxide transformations in fired clays. Journal of the American Ceramic Society, 64(5): 263–269.

McConville, C.J., and Lee, E.W. 2005. Microstructural development on firing illite and smectite clays compared with that in kaolinite. Applied Clay Science, 88(8): 2267-2276.

Onike, F.N. 1985. Time-temperature-transformation curve for and the thermal decomposition reactions of kaolinite, montmorillonite and two muscovite samples. Ph.D. Thesis, University of Hull, Hull (United Kingdom).

Pardo, F., Meseguer, S., Jordán, M.M., Sanfeliu, T., and González, I. 2011. Firing transformations of Chilean clays for the manufacture of ceramic tile bodies. Applied Clay Science, 51(1-2): 147–150.

Peters, T., and Iberg, R. 1978. Mineralogical changes during firing of calcium-rich brick clays. Ceramic Bulletin, 57(5): 503-509.

Riccardi, M.P., Messiga, B., and Duminuco, P. 1999. An approach to the dynamics of clay firing. Applied Clay Science, 15(3-4): 393–409.

Robinson, G.C. 1982. Characterization of bricks and their resistance to deterioration mechanisms. In: Conservation of Historic Stone Buildings and Monuments, National Academy Press, pp. 145-162.

Stępkowska, E.T., and Jefferis, S.A. 1992. Influence of microstructure on firing colour of clays. Applied Clay Science, 6(4): 319-342.

Swapan, K., Kausik, D., Nar, S., and Sarkar, R. 2005. Shrinkage and strength behaviour of quartzitic and kaolinitic clays in wall tile compositions. Applied Clay Science, 29(2): 137-143.

Tite, M.S., and Maniatis, Y. 1975. A scanning electron microscope examination of the bloating of fired clays. Transactions of the British Ceramic Society, 74: 229-232.

Trindade, M.J., Dias, M.I., Coroado, J., and Rocha, F. 2009. Mineralogical transformations of calcareous rich clays with firing: A comparative study between calcite and dolomite rich clays from Algarve, Portugal. Applied Clay Science, 42: 345-355.

Tuttle, O.F., and Bown, N.L. 1958. The origin of granite in the light of experimental studies in the system $NaAlSi_3O_8$-$KAlSi_3O_8SiO_2$. Geological Society of America Bulletin, 74, Baltimore, 153p.

Velandia, F., Acosta, J., Terraza, R., and Villegas, H. 2005. The current tectonic motion of the Northern Andes along the Algeciras Fault System in SW Colombia. Tectonophysics, 399: 313-329.